World Journal of Radiology

Submit a Manuscript: https://www.f6publishing.com

World J Radiol 2024 April 28; 16(4): 82-93

DOI: 10.4329/wjr.v16.i4.82

ISSN 1949-8470 (online)

ORIGINAL ARTICLE

Observational Study

Characterization of tumors of jaw: Additive value of contrast enhancement and dual-energy computed tomography

Deepak Justine Viswanathan, Ashu Seith Bhalla, Smita Manchanda, Ajoy Roychoudhury, Deepika Mishra, Asit Ranjan Mridha

Specialty type: Radiology, nuclear medicine and medical imaging

Provenance and peer review: Invited article; Externally peer reviewed.

Peer-review model: Single blind

Peer-review report's classification
Scientific Quality: Grade B
Novelty: Grade A
Creativity or Innovation: Grade A
Scientific Significance: Grade B

P-Reviewer: Zhang Z, China

Received: December 10, 2023
Revised: March 19, 2024
Accepted: April 16, 2024
Published online: April 28, 2024

Deepak Justine Viswanathan, Ashu Seith Bhalla, Smita Manchanda, Department of Radiodiagnosis and Interventional Radiology, All India Institute of Medical Sciences, New Delhi 110029, India

Ajoy Roychoudhury, Department of Oral and Maxillofacial Surgery, All India Institute of Medical Sciences, New Delhi 110029, India

Deepika Mishra, Department of Oral Pathology and Microbiology, All India Institute of Medical Sciences, New Delhi 110029, India

Asit Ranjan Mridha, Department of Pathology, All India Institute of Medical Sciences, Ansari Nagar, New Delhi 110029, India

Corresponding author: Ashu Seith Bhalla, MBBS, MD, Professor, Department of Radiodiagnosis and Interventional Radiology, All India Institute of Medical Sciences, No. 71 Ansari Nagar East, New Delhi 110029, India. ashubhalla2@gmail.com

Abstract

BACKGROUND

Currently, the differentiation of jaw tumors is mainly based on the lesion's morphology rather than the enhancement characteristics, which are important in the differentiation of neoplasms across the body. There is a paucity of literature on the enhancement characteristics of jaw tumors. This is mainly because, even though computed tomography (CT) is used to evaluate these lesions, they are often imaged without intravenous contrast. This study hypothesised that the enhancement characteristics of the solid component of jaw tumors can aid in the differentiation of these lesions in addition to their morphology by dual-energy CT, therefore improving the ability to differentiate between various pathologies.

AIM

To evaluate the role of contrast enhancement and dual-energy quantitative parameters in CT in the differentiation of jaw tumors.

METHODS

Fifty-seven patients with jaw tumors underwent contrast-enhanced dual-energy CT. Morphological analysis of the tumor, including the enhancing solid component, was done, followed by quantitative analysis of iodine concentration (IC),

water concentration (WC), HU, and normalized IC. The study population was divided into four subgroups based on histopathological analysis-central giant cell granuloma (CGCG), ameloblastoma, odontogenic keratocyst (OKC), and other jaw tumors. A one-way ANOVA test for parametric variables and the Kruskal-Wallis test for non-parametric variables were used. If significant differences were found, a series of independent *t*-tests or Mann-Whitney *U* tests were used.

RESULTS

Ameloblastoma was the most common pathology (n = 20), followed by CGCG (n = 11) and OKC. CGCG showed a higher mean concentration of all quantitative parameters than ameloblastomas ($P < 0.05$). An IC threshold of 31.35 × 100 μg/cm^3 had the maximum sensitivity (81.8%) and specificity (65%). Between ameloblastomas and OKC, the former showed a higher mean concentration of all quantitative parameters ($P < 0.001$), however when comparing unilocular ameloblastomas with OKCs, the latter showed significantly higher WC. Also, ameloblastoma had a higher IC and lower WC compared to "other jaw tumors" group.

CONCLUSION

Enhancement characteristics of solid components combined with dual-energy parameters offer a more precise way to differentiate between jaw tumors.

Key Words: Jaw neoplasms; Ameloblastomas; Dual-energy computed tomography; Iodine quantification; Mandibular neoplasms; Maxillary neoplasms

Core Tip: Quantitative dual-energy computed tomography (DECT) parameters provide a reliable way of characterizing morphologically similar jaw lesions and can serve as a single modality to differentiate jaw lesions based on their appearance and material density concentrations. In addition to providing fast imaging and material decomposition algorithms at about comparable dosage equivalency as compared to traditional computed tomography, contrast-enhanced DECT can potentially alleviate the challenge of discriminating jaw lesions without a biopsy.

Citation: Viswanathan DJ, Bhalla AS, Manchanda S, Roychoudhury A, Mishra D, Mridha AR. Characterization of tumors of jaw: Additive value of contrast enhancement and dual-energy computed tomography. *World J Radiol* 2024; 16(4): 82-93
URL: https://www.wjgnet.com/1949-8470/full/v16/i4/82.htm
DOI: https://dx.doi.org/10.4329/wjr.v16.i4.82

INTRODUCTION

Various imaging modalities are available for the evaluation of jaw lesions, the most important being panoramic radiographs, computed tomography (CT), and magnetic resonance imaging. The imaging approach towards differentiation of these lesions is mainly based on the lesion's morphology, whether lytic, sclerotic, or mixed; multilocular or unilocular; expansion; and features of aggression[1,2]. Neoplasms across the body, including solid-cystic lesions, are characterized radiologically on the basis of qualitative and quantitative evaluation of the solid component of the tumor, which forms the major component in providing a differential diagnosis. However, the literature on jaw lesions does not emphasize the characteristics of solid components. This is also because, even though CT is used in the evaluation of these lesions, most often they are imaged without intravenous contrast agents, *i.e.*, using cone beam CT scanners.

Here comes the role of contrast-enhanced CT, which makes characterization of the solid component possible and gives important information about the nature and extent of a particular tumor, helping the radiologist to give a possible range of differential diagnoses. Dual-energy CT (DECT) is an innovative technique that operates based on differential attenuation of tissues when penetrated with higher (140 kVp) and lower (80/100 kVp) energy and combines the CT attenuation-based imaging with material-specific or spectral imaging[3]. This in turn gives the added advantage of characterizing lesions based on the quantitative parameters touted to be material-specific, which can further increase the diagnostic confidence with which the radiologist conveys the possible diagnoses. The hypothesis of this study is that the enhancement characteristics of the solid component of jaw tumors is important for the differentiation of these lesions and evaluation of the same in addition to its morphology by DECT, therefore, improving the ability to differentiate between various pathologies[4-6].

MATERIALS AND METHODS

This observational study was conducted prospectively from July 2020 to April 2022 after obtaining approval by the

Institutional Ethics Committee (IECPG-354/22.07.2020, RT-2/26.08.2020). The study subjects were patients who presented with complaints of swelling in the maxilla or mandible. Patients were first screened with panoramic radiographs. Those who were found to have any lytic or sclerotic lesions in the panoramic radiographs were included. Patients without histopathological confirmation, those with uncomplicated, typical benign cysts on orthopantomography (such as radicular cysts and dentigerous cysts), clinically insignificant lesions, patients who were unwilling to participate in the study, and those who were diagnosed with other infectious conditions like osteomyelitis, traumatic lesions, or primary tumors in the oral cavity invading the jaw, were excluded. After giving their full informed consent, all patients underwent a contrast-enhanced DECT. Blood investigations were done to evaluate the renal status before administering intravenous contrast agents.

The clinical information collected was patient demographic data (age and sex) through a proforma filled out by the patient, symptomatology (including swelling, pain, bleeding, fever, tooth mobility, trismus, or any other complaints), and their duration.

Contrast-enhanced DECT imaging

Data acquisitions were performed using single-source DECT in gemstone spectral imaging (GSI) mode with a fast tube voltage switching between 80 and 140 kVp (Revolution CT, GE Healthcare, Waukesha, WI, United States). Intravenous non-ionic contrast was given at 1.0 mL/kg. Routine soft tissue and bone windows were read. Standard multiplanar reconstructions and panoramic reconstructions were made. In addition, two types of images were obtained from the reconstruction of DECT imaging automatically with GSI viewer software (GE Healthcare) for each patient: The iodine-based and water-based material decomposition (MD) images (Figure 1).

Data collection

Morphological parameters: The location of the lesion was recorded according to the bone in which it was seen. The parameters evaluated for characterization were - size, aggression, expansion, margins, matrix, cortical involvement, mandibular canal status, and relation to teeth, while cortex involvement and soft tissue extension were evaluated for extent. Based on density and locularity, the lesion was broadly divided into four subgroups: Lytic unilocular, lytic multilocular, mixed lytic-sclerotic, and sclerotic (Figure 2). Sclerotic lesions were excluded from further quantitative analysis due to the paucity of measurable soft tissue.

DECT parameters: The regions of enhancement on soft tissue windows were selected in comparison to virtual non-contrast images, and an elliptical region of interest (ROI) was placed on the most enhancing parts as assessed on monochromatic (65 kev) and iodine images. The measurements included the mean value and area of measurement (mm^2). To ensure consistency, all measurements were performed three times at different image levels, and the average values were calculated. For all measurements, the size, shape, and position of the ROI were consistent between the soft tissue images and the iodine-based MD images, as confirmed using the copy-and-paste function. Lesions with at least a soft tissue component of 1 mm^2 were selected for analysis. The iodine concentration (IC) of the lesions was measured (expressed in multiples of 100 $\mu g/cm^3$) from the iodine-based MD image, and the water concentration (WC) from the water-based MD image (expressed in multiples of 1000 mg/cm^3) along with the overlay colormap to increase the assessed lesion contrast. The normalized IC (NIC) was calculated from the ratio of the measured IC of the lesion (ICL) and the IC of the ipsilateral common carotid artery (CCA) proximal to its bifurcation (ICA) *via* the insertion of two ROIs—one in the assessed lesion and the other in the CCA. In addition to the above, an analysis of the cystic component was also made in the unilocular ameloblastomas (UA) and odontogenic keratocysts (OKCs). The parameters recorded were IC and WC.

Histopathology data-gold standard: Post-biopsy, excision, or curettage, the sampled tissue specimens were reviewed by two consultant pathologists with 10 years of experience in oral pathology. Sections from routine tissue blocks were examined using hematoxylin and eosin staining. The results were documented as ameloblastoma and non-ameloblastoma, along with the individual-specific histopathological diagnosis.

Statistical analysis

The statistical analysis for this study was done using SPSS version 28.0 software. Continuous variables (age, tumor volume, quantitative DECT, and IHC parameters) were all summarized as mean ± SD, and categorical values were summarized as proportions. The comparison of the mean ± SD between the two groups was done using an independent sample *t*-test. Categorical variables (histopathology data, patient symptomatology, and morphological parameters) were summarized as percentages. A comparison of proportions between the two groups was done using the chi-square test. Since we compared more than two independent groups for the analysis of DECT quantitative parameters, a one-way ANOVA test was performed for variables that showed a normal parametric distribution (mean HU at 65 kev, ICL, WCL) and a Kruskal-Wallis *H* test for non-parametric variables (NIC). If significant differences were discovered, we conducted a series of independent *t*-tests and Mann-Whitney *U* tests to determine the source of the difference. The value of $P < 0.05$ was considered statistically significant. The diagnostic performance was evaluated by calculating the area under the receiver operating characteristic curve (AUC).

The statistical methods of this study were reviewed by Mr. Hem Sati from the Department of Biostatistics, All India Institute of Medical Sciences, New Delhi.

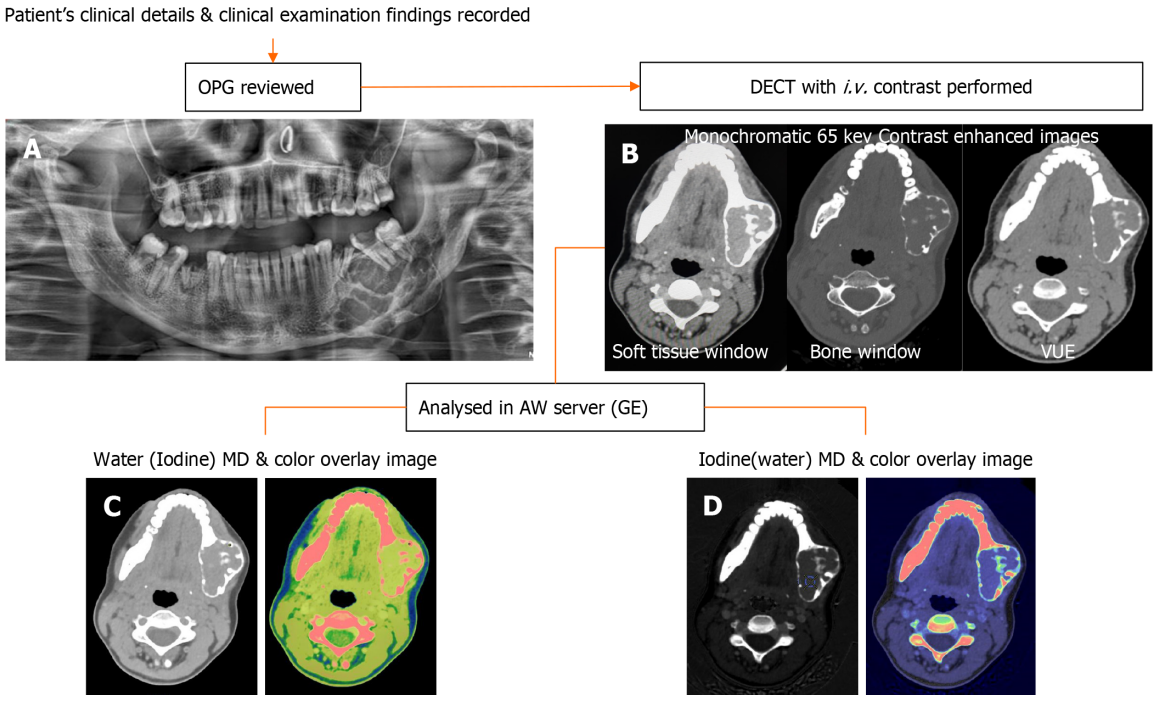

Figure 1 Workflow of patients undergoing dual-energy computed tomography Imaging. A: Orthopantomogram images are reviewed first; B: Followed by dual-energy computed tomography (DECT) acquisition using intravenous non-ionic iodinated contrast; C: Water (Iodine) with color overlay; D: Iodine (water) with color overlay are the material density images reconstructed in the dedicated software for quantitative analysis. DECT: Dual-energy computed tomography; OPG: Orthopantomography; MD: Material decomposition.

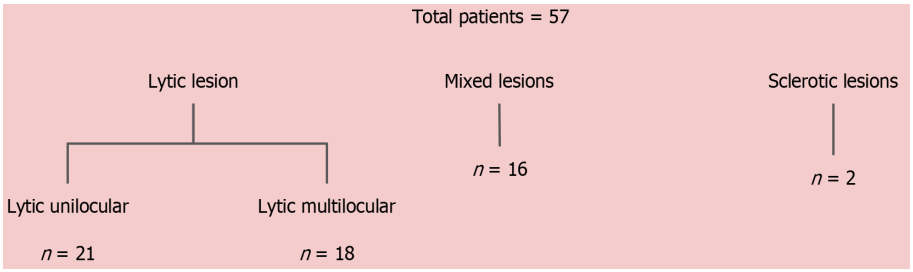

Figure 2 Classification of lesions based on computed tomography morphology (density and locularity).

RESULTS

Demographic and clinical characteristics

Fifty-seven patients (mean age, 37 ± 17 years, 26 males, and 31 females) were included in the study. The maximum number of patients was in the age group of 31-40 years (n = 14). The most common presenting complaint was swelling, which was seen in 96% of patients (n = 55), followed by local pain in 39% of patients (n = 22). The majority of the lesions (44%) were present for more than 6 months.

Histopathology results

In our study, histopathology was used as the gold standard for diagnosing jaw lesions. Twenty (35.09%) of the 57 patients had ameloblastomas, and 37 (64.91%) had non-ameloblastomas. With 11 cases, central giant cell granulomas (CGCG) were the most common lesions amongst non-ameloblastomas (29.7%). Table 1 summarizes the histopathological diagnosis of the lesions.

Morphological analysis on CECT

Of the 57 patients, 42 (73%) had lesions involving the mandible, and 13 (23%) had maxillary lesions, with thirteen patients having two lesions and two of them having three lesions. The morphological parameters were summarized for both ameloblastoma and non-ameloblastoma groups (Table 2). The ameloblastoma group showed a higher median volume (73.6 cm^3), more necrosis, a higher percentage of inferior alveolar canal involvement, retromolar trigone (RMT) involvement, and cortical involvement in the form of expansion or thinning. All these were statistically significant.

Table 1 Spectrum of lesions in histopathology

Final diagnosis	Number of lesions	Percentage (%)
Ameloblastomas	20	35
Central giant cell granuloma	11	19
Odontogenic keratocyst	6	10
Ossifying fibroma	5	8
Salivary gland tumors	2	4
Malignancy	3	5
Chondromyxoid fibroma	1	2
Non-tumorous	5	9
Sclerotic lesions	2	4
Ameloblastic fibroma	1	2
Odontogenic myxoma	1	2
Total	57	100

Table 2 Comparison of morphological characteristics between ameloblastoma and non-ameloblastoma groups

Variable	Ameloblastoma (*n* = 20)	Non-ameloblastoma (*n* = 37)	*P* value
Volume, cm^3	73.6 (7.6–1014)	39.12 (0.6–1296)	< 0.05
Cystic/necrotic areas	100	51	< 0.05
Cortical expansion/thinning	100	78	< 0.05
Mandibular canal involvement	60	32	< 0.05
Retromolar trigone involvement	45	18	< 0.05

Aggressive features evaluated in the case of mandibular tumors included mandibular canal involvement (*n* = 12), involvement of RMT (*n* = 16), condyle (*n* = 2), and coronoid process (*n* = 3). In cases of lesions in the maxilla, six cases showed aggressive features in the form of extension into the infratemporal fossa/orbit/pterygoid plates. Overall, locally aggressive features were seen in 19 cases (33%).

Quantitative analysis of solid components in contrast-enhanced DECT

On a broad comparison between the ameloblastoma and non-ameloblastoma groups, the ameloblastomas had a higher mean IC, a higher mean HU at 65 kev, a lower average NIC, and a lower WC compared to the non-ameloblastomas.

The ameloblastomas mostly had IC s in the 16–30 (moderate) mmol/mm^3 range and mean attenuation in the range of 50–150 HU. In contrast, 90% of CGCGs showed ICs greater than 31 mmol/mm^3 and mean attenuation > 150 HU. The OKCs had low values in all the parameters, distinctly different from others. The rest of them did not show any significant difference between them in their respective groups (Table 3). This could be attributed to the heterogeneous sample within the non-ameloblastoma group, which included cystic lesions with virtually no enhancing solid component and avidly enhancing masses. Statistical analysis revealed that the values of DECT parameters in OKCs and CGCCs were on the extreme opposite spectrum, with other lesions having values in between. Hence, we further subdivided the non-ameloblastoma group into three sub-groups and compared ameloblastomas with these three subgroups: OKCs, CGCG, and other jaw tumors.

Comparison between ameloblastoma and three major subgroups within the non-ameloblastoma group (Table 4):

When we compared ameloblastoma and central giant cell granuloma lesions (*n* = 31), significant differences were found in all quantitative DECT parameters ($P < 0.05$). CGCGs showed a higher average iodine content (36.1 × 100 *vs* 29.8 × 100 µg/cm^3), higher average WC (1042 × 1000 *vs* 1032 × 1000 mg/cm^3), a higher mean HU at 65 Kev (151 *vs* 122 HU), and a higher NIC (0.59 *vs* 0.34) compared to ameloblastomas (Figure 3).

In comparison between ameloblastomas and OKCs (*n* = 26), both groups showed significant differences in all the DECT parameters. However, the diagnostic dilemma lies in the distinction between UA and OKCs, which appear similar in morphology on conventional CT. Hence, to make this comparison impactful, we compared the WC of the cystic component in addition to the DECT parameters mentioned above between UA and OKCs. Interestingly, in addition to the above quantitative parameters, which were statistically significant, the WC of the cystic component also showed statistically significant differences between the two subgroups (Figure 4). In the OKCs, significantly higher water content within the cystic component was observed compared to ameloblastomas. When the ameloblastomas were compared with

Table 3 Classification of lesions based on iodine concentration (μg/mL)

Iodine concentration (μg/mL)	0-15 (low)	16-30 (moderate)	31-45 (high)	≥ 46 (extreme)
Ameloblastoma	2	11	4	1
CGCG	0	1	8	0
OKC	5	0	0	0
OF	0	3	0	0
Salivary gland tumor	1	1	0	0
Chondromyxoid fibroma	0	0	0	1
Others	4	6	2	1

All odontogenic keratocysts had a lower iodine concentration (0-15). Ameloblastomas predominantly had a moderate iodine concentration (16-30). Central giant cell granuloma predominantly had a higher iodine concentration (31-45). OKC: Odontogenic keratocysts; OF: Ossifying fibromas; CGCG: Central giant cell granuloma.

Table 4 Comparison of dual-energy computed tomography quantitative parameters between subgroups

Parameters	Amelo, mean ± SD	OKC, mean ± SD	CGCG, mean ± SD	Other JT, mean ± SD	[1]*P* value	[2]*P* value	[3]*P* value
Mean HU	122 ± 28.3	33 ± 12.4	151 ± 24.3	117 ± 37.9	0.007	< 0.001	0.616
IC	29 ± 9.3	7.2 ± 5.8	36.1 ± 6.8	24.8 ± 11.5	0.036	< 0.001	0.232
WC	1032.5 ± 13	1010 ± 11	1043 ± 11.6	1040 ± 11.4	0.036	0.044	0.056
NIC	0.35 ± 0.15	0.10 ± 0.1	0.59 ± 0.25	0.39 ± 0.24	0.011	0.007	0.501
WC (cystic)	997 ± 5.6	1020 ± 5	-	-	-	< 0.001	-

[1]*P* value obtained on comparison between ameloblastomas and central giant cell granulomas.
[2]*P* value obtained when unilocular ameloblastomas were compared with odontogenic keratocysts.
[3]*P* value obtained when ameloblastomas were compared with other jaw tumors.
Mean HU is the mean computed tomography density expressed in Hounsfield units. IC is the Iodine concentration of solid enhancing component expressed in 100 μg/cm^3. WC is the water concentration of solid enhancing component expressed in 1000 mg/cm^3. NIC is the normalized iodine concentration calculated as a ratio. WC (cystic) is the water concentration of cystic component calculated only in cases of unilocular ameloblastomas and OKCs. Other jaw tumor are a subgroup of lesions excluding ameloblastoma, CGCG and OKCs. IC: Iodine concentration; WC: Water concentration; NIC: Normalized iodine concentration; OKC: Odontogenic keratocyst; JT: Jaw tumor; CGCG: Central giant cell granuloma.

the "other jaw tumor" group, the former showed a higher average iodine content, although not statistically significant, and a lower WC, which was marginally significant compared to the latter (Figure 5).

Receiver operating characteristic analysis for calculating threshold values

The comparison of ameloblastomas and CGCG yielded statistically significant differences and satisfied the sample size for receiver operating characteristic (ROC) analysis. Hence, ROC analysis for all the DECT parameters was performed, and based on the AUC values, we selected a threshold for each parameter with the largest areas under the ROC curves (Table 5).

DECT evaluation of lesions based on morphology

Because the majority of jaw lesions are diagnosed using a systematic approach based on morphological appearance, we attempted to categorize the lesions based on density and locularity as described above and then studied their DECT parameters, except for the sclerotic lesions. The mean values of the DECT parameters of the lesions in the different morphological subgroups are summarized in Table 6.

DISCUSSION

We performed contrast-enhanced DECT with a predetermined split bolus contrast protocol in 57 patients with suspected maxillary and/or mandibular tumors or neoplasms after obtaining proper written informed consent, reviewing the clinical details, physical examination findings, and orthopantomogram. The morphological and quantitative spectral parameters obtained from DECT imaging were evaluated for the differentiation of various tumors of the jaw. The

Table 5 Receiver operating characteristic analysis of dual-energy computed tomography parameters between ameloblastoma and central giant cell granulomas

Variable	Cutoff value	Sensitivity, %	Specificity, %	AUC	SE
IC	32.1	81.82	65.00	0.727	0.0955
Mean HU	134	81.82	65.00	0.789	0.0832
WC	1036	72.73	50.00	0.6659	0.1
NIC	0.4	81.82	70.00	0.795	0.0970

Mean HU is the mean computed tomography density expressed in Hounsfield units. IC: Iodine concentration; WC: Water concentration; NIC: Normalized iodine concentration; AUC: The area under the receiver operating characteristic curve.

Table 6 Comparison of dual-energy computed tomography quantitative parameters based on morphology

Lytic unilocular (*n* = 21)	**Amelo, *n* = 7 (mean ± SD)**	**OKC, *n* = 6 (mean ± SD)**	**CGCG, *n* = 2 (mean ± SD)**	**OF, *n* = 2 (mean ± SD)**	**Non-tumorous, *n* = 4 (mean ± SD)**
Mean HU	115 ± 18.3	33 ± 12.4	135 ± 24	87 ± 17.9	67 ± 17.9
IC	28 ± 8.3	7.2 ± 5.8	32.9 ± 6.8	18.8 ± 9.5	8.8 ± 9.5
WC	1030.5 ± 12.8	1010 ± 11.3	1043 ± 11.6	1038 ± 11.4	1018 ± 11.4
NIC	0.37 ± 0.15	0.10 ± 0.1	0.72 ± 0.3	0.45 ± 0.24	0.25 ± 0.24
Lytic multilocular (*n* = 18)	**Amelo, *n* = 8 (mean ± SD)**	**CGCG, *n* = 4 (mean ± SD)**	**SG tumors, *n* = 2 (mean ± SD)**	**Malignancy, *n* = 3 (mean ± SD)**	**Non-tumorous, *n* = 1 (mean ± SD)**
Mean HU	123 ± 21.3	152 ± 20.4	94.2 ± 24.3	120 ± 37.9	69 ± 18.9
IC	29 ± 9.3	35.1 ± 9.8	17.85 ± 6.8	24.8 ± 11.5	10 ± 2.5
WC	1032.5 ± 12.8	1048 ± 11.3	1038 ± 11.6	1040 ± 11.4	1011 ± 11.4
NIC	0.35 ± 0.15	0.54 ± 0.19	0.18 ± 0.05	0.39 ± 0.24	0.29 ± 0.1
Mixed-sclerotic (*n* = 16)	**Amelo, *n* = 5 (mean ± SD)**	**CGCG, *n* = 5 (mean ± SD)**	**OFs, *n* = 4 (mean ± SD)**	**CMF, *n* = 1 (mean ± SD)**	**Non-tumorous, *n* = 1 (mean ± SD)**
Mean HU	129 ± 20.3	158 ± 20.4	143.8 ± 24.3	164 ± 37.9	77 ± 16
IC	29.5 ± 9.3	38.2 ± 9.8	31.1 ± 6.8	49.8 ± 11.5	11.8 ± 9
WC	1032.5 ± 12.8	1048 ± 11.3	1043 ± 11.6	1037 ± 11.4	1028 ± 20.4
NIC	0.35 ± 0.15	0.60 ± 0.19	0.66 ± 0.25	0.37 ± 0.24	0.19 ± 0.14

Amelo: Ameloblastoma; OKC: Odontogenic keratocysts; OF: Ossifying fibromas; CGCG: Central giant cell granuloma; SG tumors: Salivary gland tumors; IC: Iodine concentration; WC: Water concentration; NIC: Normalized iodine concentration; CMF: Chondromyxoid fibroma

primary goal of the study was to identify qualitative and quantitative parameters for distinguishing ameloblastomas from non-ameloblastomas.

There was a slight female predominance and the majority, *i.e.*, 77% of non-ameloblastomas comprised females compared to 35% in the ameloblastoma group. We studied the morphological features of lesions, and a comparison was made between the ameloblastoma and non-ameloblastoma groups. Median volume, degree of necrosis, inferior alveolar canal involvement, RMT involvement, and cortical involvement in the form of expansion or thinning were significantly higher in the ameloblastoma group. Our study agrees with these characteristics of ameloblastomas in other studies done previously in larger populations[7-10]. However, when the location was maxilla, there was no significant difference between the two groups. The rest of the variables, *i.e.*, margins, relation to teeth, and soft tissue extension, showed no statistically significant difference between the two groups.

In this study, we also investigated the potential of using quantitative information provided by both the virtual monochromatic images and MD images in dual-energy spectral CT imaging for the differentiation of ameloblastomas and non-ameloblastomas. Iodine, as the main component of a contrast medium, allows the assessment of vascular beds and intercellular spaces, and it facilitates the differentiation of lesions at various locations in the body based on the assumption that malignant, aggressive, or vascular lesions exhibit a higher degree of contrast enhancement[11]. DECT allows the quantitative assessment of the concentration of iodine accumulated in a unit of tissue volume. The degree of angiogenesis indicates the degree of viability, the degree of malignancy, and the vascularization sources[5,12]. Although there were no studies evaluating the role of DECT in jaw tumors, various studies done elsewhere in the head and region

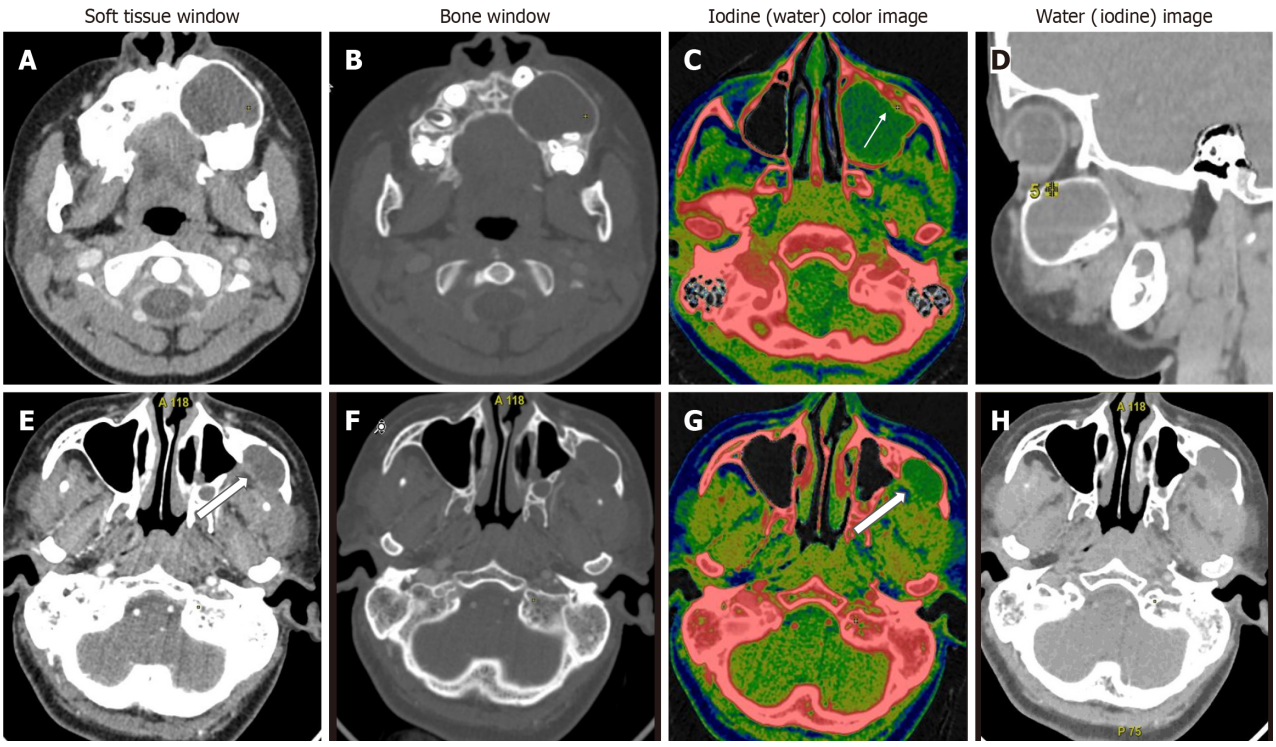

Figure 3 Unilocular lytic lesions differentiated based on water concentration. A-D: Unilocular ameloblastoma - contrast-enhanced dual-energy computed tomography images show a well-defined lytic unilocular cystic, expansile lesion in the left maxilla with mild peripheral rim enhancement better appreciated on iodine colour overlay images (white arrow). Water (iodine) material decomposition (MD) images showed a WC of 986 μg/cm^3 in the cystic component; E-H: Odontogenic keratocyst is also a well-defined lytic, unilocular cystic, expansile lesion in the left lateral wall of the maxillary sinus with a small enhancing mural component posteriorly (white open arrows). Water (Iodine) MD images revealed a water concentration of 1045 μg/cm^3 in the cystic component. In this case, due to the paucity of soft tissue components, iodine concentration did not help; however, the water concentration of the cystic component differed significantly, aiding in the diagnosis.

showed MD images, especially IC images, can be used for the differentiation of various pathologies[4]. This was because it is now known that the IC value is more accurate than the CT value in assessing the blood supply to a lesion.

The higher IC in ameloblastomas can be attributed to the fact that these are slow-growing, locally invasive tumors with an explicit biologic pattern. Multiple stromal factors, including growth and angiogenic factors, extracellular matrix components, and proteinases, are overexpressed and linked to the development of this tumor, where they play critical roles in invasion, growth, and progression with aggressive behavior. This could explain the rise in metabolic activity in ameloblastoma connective tissue[13-16]. The non-ameloblastomas included a heterogeneous sample within the group that ranged from cystic lesions with enhancing wall/septae and virtually no enhancing mural component like OKCs to avidly enhancing solid lesions like CGCGs. This was also supported by the fact that statistical analysis revealed that the values of DECT parameters in OKCs and CGCCs were on the extreme opposite spectrum, with other lesions having values ranging in between. This led to further classification of the non-ameloblastomas and their comparison with ameloblastomas.

On the first comparison between ameloblastomas and CGCG, the CGCGs had higher mean iodine, water, mean HU at 65 Kev, and NIC compared to ameloblastomas. This was in accordance with the earlier studies, which showed that central giant cell lesions had significantly higher angiogenetic potential compared to ameloblastomas[17,18]. The differential analysis based on the calculated threshold IC value showed that a value of 32.1 × 100 μg/cm^3, best represented the differences based on the AUC values on the ROC curves, with a sensitivity and specificity of 81.8% and 65%, respectively.

In a comparison of ameloblastomas with OKCs, similar to morphological features, all quantitative parameters showed significant differences between the two lesions in our study[19]. Interestingly, in addition to the DECT quantitative parameters of enhancing components, the WC of the cystic component also showed a statistically significant difference between the two subgroups. In the OKCs, significantly higher water content within the cystic component was observed compared to ameloblastomas (1020 *vs* 997 μg/cm^3). Our study showed that UA and OKCs could be effectively differentiated on the basis of the IC and WC measurements of the cystic component, as these lesions are often purely cystic (Figure 4). Our finding that the WC of the cystic areas differs significantly between the ameloblastomas and OKCs indicates that the density of the cystic components with suppressed iodine information varies between these odontogenic tumors. Cystic spaces in the ameloblastomas usually contain slightly proteinaceous fluids, occasionally associated with colloidal materials[20]. The cyst lumen of OKCs often contains desquamated keratin. This desquamated keratin accumulates in such large quantities that it influences the attenuations on CT images, which was even proven in an experimental study by Yoshiura *et al*[21]. Therefore, it is plausible that such desquamated keratin increased the viscosity of fluids in the lumen, thereby increasing the value of WC in the water (iodine) images compared with ameloblastomas, in which increases in viscosity may be minimal.

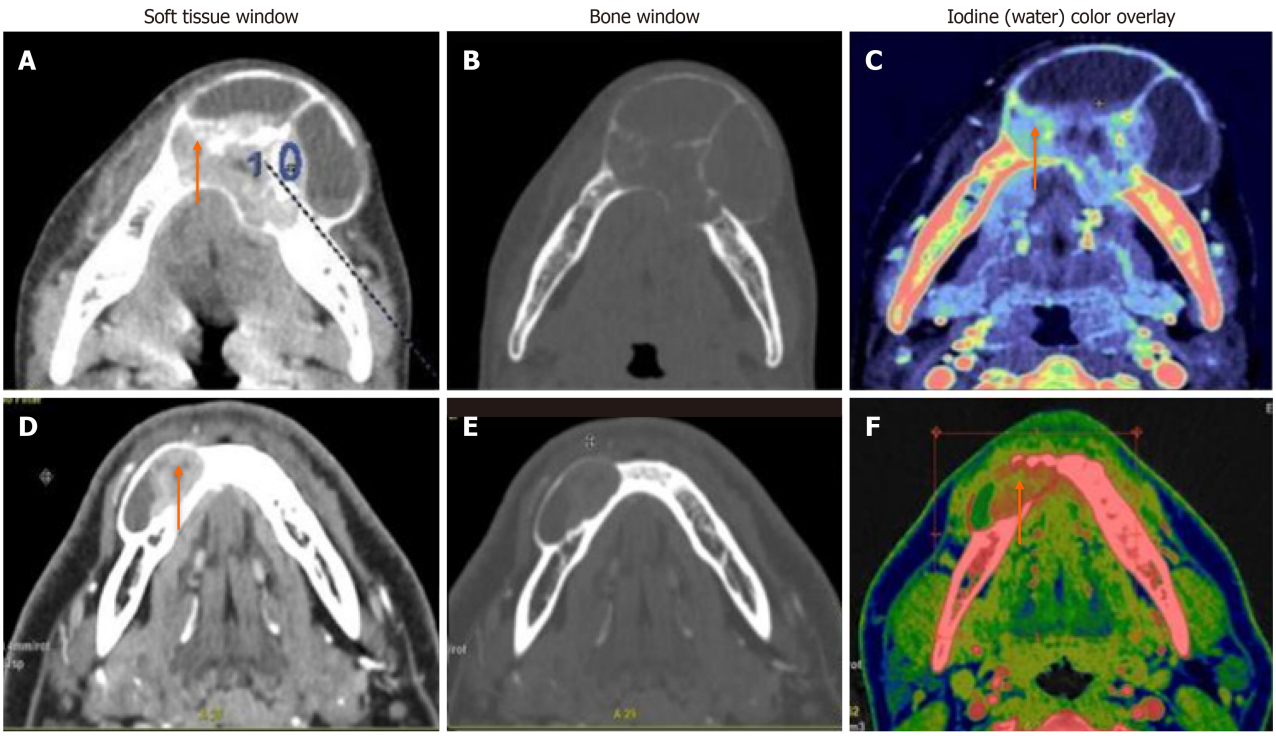

Figure 4 Multilocular solid-cystic lesions differentiated based on iodine concentration. A-C: Central giant cell granuloma - A well-defined expansile multiloculated solid-cystic tumor in the left anterior mandible crossing the midline. Iodine images with a color overlay (C) showed an iodine concentration (IC) of 57 × 100 μg/cm^3 of the solid enhancing part (orange arrow); D-F: Ameloblastoma - a well-defined lytic, unilocular, solid-cystic, expansile lesion with an enhancing soft tissue component (orange arrow). Iodine images with a color overlay (F) show increased iodine content (areas in red) within the soft tissue (IC of 23 × 100 μg/cm^3).

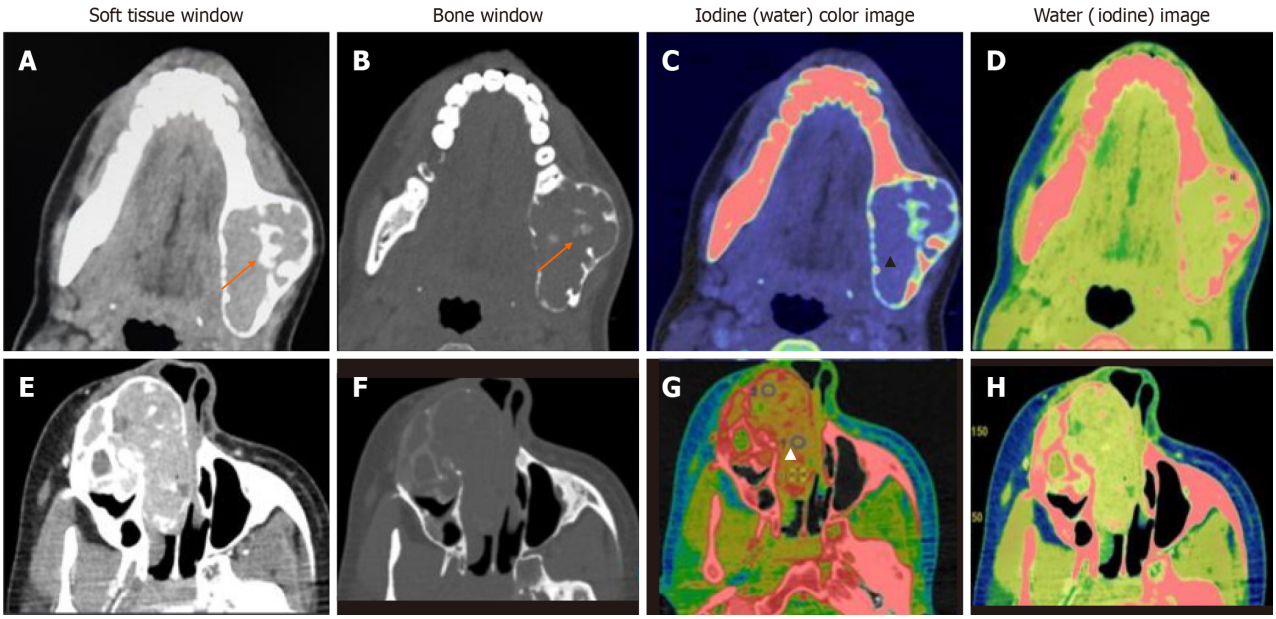

Figure 5 Mixed lytic-sclerotic lesions. A-D: Central giant cell granuloma well-defined, mixed lytic-sclerotic buccolingual expansile lesion with a narrow zone of transition. Central ossific foci are seen (orange arrows). Iodine (water) material decomposition overlay images show a mild, homogeneous iodine concentration (blue region within the tumor - black arrowhead) (C). Water (Iodine) images show no cystic or necrotic areas (D); E-H: Ossifying fibroma well- defined expansile mass epicentered in the right maxilla, showing heterogeneous enhancement in its lytic soft tissue component with multiple sclerotic foci extending into the nasal cavity (E). The iodine image shows foci of increased iodine concentration (red areas - white arrowhead) (G). Lower iodine concentration and higher water concentration were seen in the latter, which suggested “other jaw tumor” as in this case.

The above comparisons yielded an interesting fact: Ameloblastomas showed significantly increased values of DECT parameters, which were indirect markers of vascularity, compared to non-ameloblastomas except for the CGCG. As we can see, the latter has a significantly increased IC, mean HU value, WC, and NIC compared to ameloblastomas. The flowchart (Figure 6) presents an algorithmic approach to classifying jaw lesions based on differences in DECT quantitative parameters in our study.

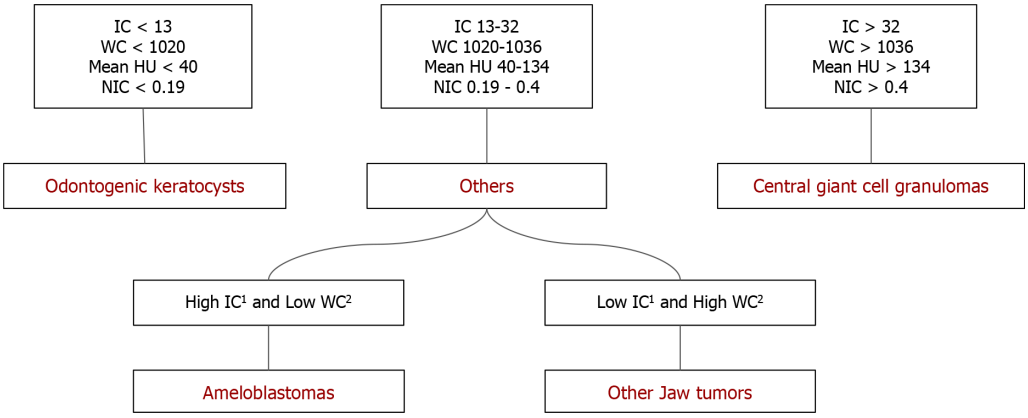

Figure 6 Flowchart showing algorithmic differentiation of jaw tumors in the study population based on the quantitative analysis. Central giant cell granulomas had higher iodine concentration (IC), water concentration (WC), and normalized IC (NIC), odontogenic keratocysts with lower IC, WC, and NIC, ameloblastomas and other jaw tumor group showed values in between. Between the two, ameloblastomas had higher IC with lower WC while other jaw tumor group had lower IC with higher WC. [1]Not significant; [2]Marginally significant. WC: Water concentration; IC: Iodine concentration; NIC: Normalized iodine concentration.

The major limitation of the present study was the heterogeneous sample within the "other jaw tumor" group, which resulted in a limited comparison of separate pathological lesions. Another limitation was the inability to compare the DECT parameters based on the morphological subgroups due to the limited sample size.

CONCLUSION

We propose that DECT can help with both morphological and functional classification of jaw tumors, as well as distinguish between various jaw tumors that closely resemble each other in conventional imaging. Our study contributes to the existing body of literature, confirming the technical feasibility of single-source spectral CT imaging, which relies on the differentiation of iodine and water, as a valuable tool for quantitatively distinguishing ameloblastoma from other jaw tumors at about comparable dose equivalency of traditional CT. Additionally, our research marks the pioneering use of DECT in characterizing and differentiating various jaw tumors.

ACKNOWLEDGEMENTS

Faculty, residents, and radiographers of the Department of Radiodiagnosis and Interventional Radiology, All India Institute of Medical Sciences, New Delhi for their support and assistance. Mr. Hem Sati, Department of Biostatistics, AIIMS, New Delhi, for biostatistical guidance.

FOOTNOTES

Author contributions: Viswanathan DJ, Bhalla AS and Manchanda S designed the research study; Viswanathan DJ performed the research; Roychoudhury A contributed to referral of cases and surgical input; Mishra D and Mriddha AR contributed to histopathological analysis and pathological insight; Viswanathan DJ analyzed the data and wrote the manuscript; All authors have read and approved the final manuscript.

Institutional review board statement: The study was reviewed and approved by the All India Institute of Medical Sciences, New Delhi Institutional Review Board (No. IECPG-354/22.07.2020, RT-2/26.08.2020).

Informed consent statement: All patients give their full informed consent.

Conflict-of-interest statement: All the authors report no relevant conflicts of interest for this article.

Data sharing statement: Technical appendix, statistical code, and dataset available from the corresponding author at ashubhalla2@gmail.

com. Participants gave informed consent for data sharing.

STROBE statement: The authors have read the STROBE Statement—checklist of items, and the manuscript was prepared and revised according to the STROBE Statement—checklist of items.

Country/Territory of origin: India

ORCID number: Deepak Justine Viswanathan 0000-0001-8169-6115; Ashu Seith Bhalla 0000-0003-2200-2544.

S-Editor: Li L
L-Editor: A
P-Editor: Zhao S

REFERENCES

1 **Soluk-Tekkeşin M**, Wright JM. The World Health Organization Classification of Odontogenic Lesions: A Summary of the Changes of the 2017 (4th) Edition. *Turk Patoloji Derg* 2018; **34** [PMID: 28984343 DOI: 10.5146/tjpath.2017.01410]
2 **Dunfee BL**, Sakai O, Pistey R, Gohel A. Radiologic and pathologic characteristics of benign and malignant lesions of the mandible. *Radiographics* 2006; **26**: 1751-1768 [PMID: 17102048 DOI: 10.1148/rg.266055189]
3 **McCollough CH**, Leng S, Yu L, Fletcher JG. Dual- and Multi-Energy CT: Principles, Technical Approaches, and Clinical Applications. *Radiology* 2015; **276**: 637-653 [PMID: 26302388 DOI: 10.1148/radiol.2015142631]
4 **Roele ED**, Timmer VCML, Vaassen LAA, van Kroonenburgh AMJL, Postma AA. Dual-Energy CT in Head and Neck Imaging. *Curr Radiol Rep* 2017; **5**: 19 [PMID: 28435761 DOI: 10.1007/s40134-017-0213-0]
5 **Tawfik AM**, Razek AA, Kerl JM, Nour-Eldin NE, Bauer R, Vogl TJ. Comparison of dual-energy CT-derived iodine content and iodine overlay of normal, inflammatory and metastatic squamous cell carcinoma cervical lymph nodes. *Eur Radiol* 2014; **24**: 574-580 [PMID: 24081649 DOI: 10.1007/s00330-013-3035-3]
6 **Luo S**, Sha Y, Wu J, Lin N, Pan Y, Zhang F, Huang W. Differentiation of malignant from benign orbital tumours using dual-energy CT. *Clin Radiol* 2022; **77**: 307-313 [PMID: 35094818 DOI: 10.1016/j.crad.2021.12.019]
7 **MacDonald-Jankowski DS**, Yeung R, Lee KM, Li TK. Odontogenic myxomas in the Hong Kong Chinese: clinico-radiological presentation and systematic review. *Dentomaxillofac Radiol* 2002; **31**: 71-83 [PMID: 12076060 DOI: 10.1038/sj.dmfr.4600678]
8 **Wu PC**, Chan KW. A survey of tumours of the jawbones in Hong Kong Chinese: 1963-1982. *Br J Oral Maxillofac Surg* 1985; **23**: 92-102 [PMID: 3158339 DOI: 10.1016/0266-4356(85)90058-0]
9 **Reichart PA**, Philipsen HP, Sonner S. Ameloblastoma: biological profile of 3677 cases. *Eur J Cancer B Oral Oncol* 1995; **31B**: 86-99 [PMID: 7633291 DOI: 10.1016/0964-1955(94)00037-5]
10 **Siar CH**, Lau SH, Ng KH. Ameloblastoma of the jaws: a retrospective analysis of 340 cases in a Malaysian population. *J Oral Maxillofac Surg* 2012; **70**: 608-615 [PMID: 21723654 DOI: 10.1016/j.joms.2011.02.039]
11 **Sanghavi PS**, Jankharia BG. Applications of dual energy CT in clinical practice: A pictorial essay. *Indian J Radiol Imaging* 2019; **29**: 289-298 [PMID: 31741598 DOI: 10.4103/ijri.IJRI_241_19]
12 **Li L**, Zhao Y, Luo D, Yang L, Hu L, Zhao X, Wang Y, Liu W. Diagnostic value of single-source dual-energy spectral computed tomography in differentiating parotid gland tumors: initial results. *Quant Imaging Med Surg* 2018; **8**: 588-596 [PMID: 30140621 DOI: 10.21037/qims.2018.07.07]
13 **Chi AC**, Neville BW. Odontogenic Cysts and Tumors. *Surg Pathol Clin* 2011; **4**: 1027-1091 [PMID: 26837786 DOI: 10.1016/j.path.2011.07.003]
14 **Ribeiro BF**, Iglesias DP, Nascimento GJ, Galvão HC, Medeiros AM, Freitas RA. Immunoexpression of MMPs-1, -2, and -9 in ameloblastoma and odontogenic adenomatoid tumor. *Oral Dis* 2009; **15**: 472-477 [PMID: 19522745 DOI: 10.1111/j.1601-0825.2009.01575.x]
15 **Wang A**, Zhang B, Huang H, Zhang L, Zeng D, Tao Q, Wang J, Pan C. Suppression of local invasion of ameloblastoma by inhibition of matrix metalloproteinase-2 in vitro. *BMC Cancer* 2008; **8**: 182 [PMID: 18588710 DOI: 10.1186/1471-2407-8-182]
16 **Jamshidi S**, Zargaran M, Baghaei F, Shojaei S, Zare Mahmoodabadi R, Dehghan A, Moghimbeigi A. An Immunohistochemical Survey to Evaluate the Expression of CD105 and CD34 in Ameloblastoma and Odontogenic Keratocyst. *J Dent (Shiraz)* 2014; **15**: 192-198 [PMID: 25469359]
17 **Ali K**, Zeb Khan S, Sultana N, Alghamdi O, Muhammad S, Mokeem SA, Ali S, Abduljabbar T, Vohra F. Assessment of Tumor Angiogenesis by Expression of CD 105 in Ameloblastoma, Odontogenic Keratocyst and Central Giant Cell Lesion. *Asian Pac J Cancer Prev* 2020; **21**: 3373-3379 [PMID: 33247698 DOI: 10.31557/APJCP.2020.21.11.3373]
18 **Ghosh A**, Lakshmanan M, Manchanda S, Bhalla AS, Kumar P, Bhutia O, Mridha AR. Contrast-enhanced multidetector computed tomography features and histogram analysis can differentiate ameloblastomas from central giant cell granulomas. *World J Radiol* 2022; **14**: 329-341 [PMID: 36186516 DOI: 10.4329/wjr.v14.i9.329]
19 **Hayashi K**, Tozaki M, Sugisaki M, Yoshida N, Fukuda K, Tanabe H. Dynamic multislice helical CT of ameloblastoma and odontogenic keratocyst: correlation between contrast enhancement and angiogenesis. *J Comput Assist Tomogr* 2002; **26**: 922-926 [PMID: 12488736 DOI: 10.1097/00004728-200211000-00011]
20 **Smoker WR**, Harnsberger HR. Differential diagnosis of head and neck lesions based on their space of origin. 2. The infrahyoid portion of the neck. *AJR Am J Roentgenol* 1991; **157**: 155-159 [PMID: 2048511 DOI: 10.2214/ajr.157.1.2048511]

21 **Yoshiura K**, Higuchi Y, Ariji Y, Shinohara M, Yuasa K, Nakayama E, Ban S, Kanda S. Increased attenuation in odontogenic keratocysts with computed tomography: a new finding. *Dentomaxillofac Radiol* 1994; **23**: 138-142 [PMID: 7530666 DOI: 10.1259/dmfr.23.3.7530666]

Published by **Baishideng Publishing Group Inc**
7041 Koll Center Parkway, Suite 160, Pleasanton, CA 94566, USA
Telephone: +1-925-3991568
E-mail: office@baishideng.com
Help Desk: https://www.f6publishing.com/helpdesk
https://www.wjgnet.com